

Article

Design, Synthesis and Antifungal Evaluation of Novel Pyrylium Salt In Vitro and In Vivo

Yue Zhang ^{1,†}, Qiu hao Li ^{1,†}, Wen Chao ^{2,†}, Yulin Qin ³, Jiayan Chen ¹, Yingwen Wang ¹, Runhui Liu ^{1,*}, Quanzhen Lv ^{1,*} and Jinxin Wang ^{1,*} 

¹ School of Pharmacy, Naval Medical University, Shanghai 200433, China; yzhang_moon@163.com (Y.Z.); lqh20191034@163.com (Q.L.); chenjiayan_alice@outlook.com (J.C.); wyw20010625@163.com (Y.W.)

² Experimental Teaching Center of Basic Medicine College, Navel Medical University, Shanghai 200433, China; chaowen_2010@163.com

³ Fudan University Minhang Hospital, Shanghai 201199, China; qinyulin1990@126.com

* Correspondence: lyliurh@126.com (R.L.); lvquanzhen2011@163.com (Q.L.); jxwang2013@126.com (J.W.)

† These authors contributed equally to this work.

Abstract: Nowadays, discovering new skeleton antifungal drugs is the direct way to address clinical fungal infections. Pyrylium salt **SM21** was screened from a library containing 50,240 small molecules. Several studies about the antifungal activity and mechanism of **SM21** have been reported, but the structure–activity relationship of pyrylium salts was not clear. To explore the chemical space of antifungal pyrylium salt **SM21**, a series of pyrylium salt derivatives were designed and synthesized. Their antifungal activity and structure-activity relationships (SAR) were investigated. Compared with **SM21**, most of the synthesized compounds exhibited equivalent or improved antifungal activities against *Candida albicans* in vitro. The synthesized compounds, such as **XY10**, **XY13**, **XY14**, **XY16** and **XY17** exhibited comparable antifungal activities against *C. albicans* with MIC values ranging from 0.47 to 1.0 μ M. Fortunately, a compound numbered **XY12** showed stronger antifungal activities and lower cytotoxicity was obtained. The MIC of compound **XY12** against *C. albicans* was 0.24 μ M, and the cytotoxicity decreased 20-fold as compared to **SM21**. In addition, **XY12** was effective against fluconazole-resistant *C. albicans* and other pathogenic *Candida* species. More importantly, **XY12** could significantly increase the survival rate of mice with a systemic *C. albicans* infection, which suggested the good antifungal activities of **XY12** in vitro and in vivo. Our results indicated that structural modification of pyrylium salts could lead to the discovery of new antifungal drugs.

Keywords: pyrylium salt; SM21; antifungal; *Candida albicans*; drug discovery



Citation: Zhang, Y.; Li, Q.; Chao, W.; Qin, Y.; Chen, J.; Wang, Y.; Liu, R.; Lv, Q.; Wang, J. Design, Synthesis and Antifungal Evaluation of Novel Pyrylium Salt In Vitro and In Vivo. *Molecules* **2022**, *27*, 4450. <https://doi.org/10.3390/molecules27144450>

Academic Editor: Mads Hartvig Clausen

Received: 8 June 2022

Accepted: 7 July 2022

Published: 12 July 2022

Publisher's Note: MDPI stays neutral with regard to jurisdictional claims in published maps and institutional affiliations.



Copyright: © 2022 by the authors. Licensee MDPI, Basel, Switzerland. This article is an open access article distributed under the terms and conditions of the Creative Commons Attribution (CC BY) license (<https://creativecommons.org/licenses/by/4.0/>).

1. Introduction

Candida, *Aspergillus* and *Cryptococcus* are the main opportunistic pathogens leading to human fungal infections [1]. During the last three decades, invasive fungal infections (IFIs) have killed about 1.6 million people each year and pose a serious threat to human health, especially among people with HIV infection, cancer, organ transplants and autoimmune diseases [2]. In recent years, systemic *Candida* infection has risen to fourth place among the nosocomial blood-borne infections [3,4]. At the same time, the mortality rate of candidemia is high. According to the statistics, the 90-day mortality rate of solid-organ transplant recipients with candidiasis is 22–44% [5]. These studies indicate that pathogenic fungi are a serious and increasing threat to human health. Solving the problem of fungal infections is an important means to improve the recovery rate of patients with immunodeficiencies [6].

Despite advances in antifungal therapy, invasive fungal infection remains the major cause of morbidity and death among immunocompromised patients [7]. Clinically, three major classes of drugs are available, which include azoles, echinocandins and polyenes, but the mortality of patients with invasive fungal infection is still as high as 40% [8,9]. In addition, the long-term use of antifungal drugs causes the problem of drug resistance.

Multi-center investigations of candidiasis in China showed that about 0.5–2.0% of *C. albicans* was resistant to fluconazole. Moreover, the survival time of patients infected with drug-resistant *C. albicans* was significantly lower than that of patients infected with sensitive strains [10]. With continuous emergence of drug resistance and the undesired side effects of available antifungal drugs, effective agents with new structures and targets are urgently needed.

In 2014, Wong et al screened 50,240 compounds for their antifungal activities using the yeast-to-hyphae inhibitory phenotype. Among them, lipophilic pyrylium salt **SM21** (Figure 1 XY2 in this study) showed good antifungal activities in vitro and in vivo [11]. Related mechanistic studies demonstrate that **SM21** could inhibit the function and fusion of mitochondria in *C. albicans* [12,13]. However, the structure–activity relationship of **SM21** is not clear. In our studies, a series of pyrylium salts were rationally designed and synthesized based on the chemical space investigation of XY2 (Figure 1). The structure–activity relationship of pyrylium salts was preliminarily discussed and a compound numbered XY12 was obtained, which showed stronger antifungal activity and lower cytotoxicity. Our research provided a new lead compound for the development of antifungal drugs.

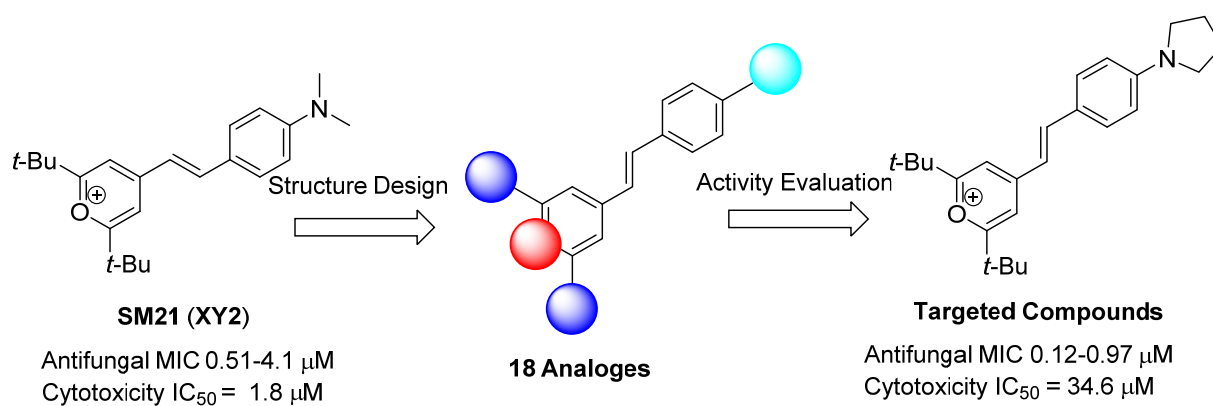
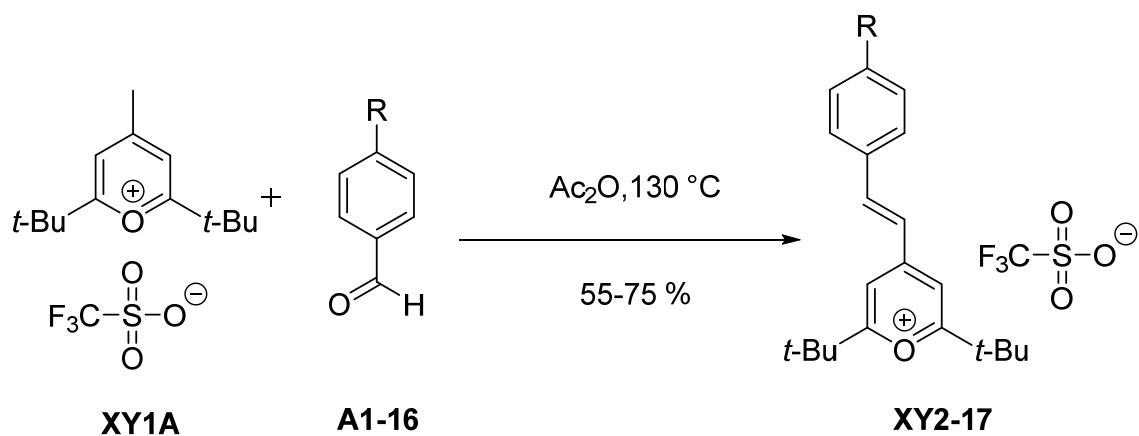


Figure 1. Design and evaluation of new antifungal agents based on lead compound **SM21** (XY2).

2. Results and Discussion

2.1. Chemistry

Except for commercially available pyrylium salt derivatives, new pyrylium salt derivatives **XY3–20** were synthesized from **XY1A** or **XY1B** (Figure 1). The synthesis of the target compounds **XY3–17**, **XY19** and **XY20** was shown in Schemes 1–3, respectively. Pyrylium salts were used as cationic dyes [14] and the methods to prepare these types of compounds were reported [15]. The target compounds **XY3–17** and **XY19** can be obtained efficiently by a dehydration condensation reaction of methyl pyrylium salt **XY1A** or **XY1B** and a different substituted aldehyde **A1–16** under the heating condition in acetic anhydride, with single trans-olefin selectivity (Schemes 1 and 2). The structures of new pyrylium salts were determined by the high resolution mass spectra and ^1H , ^{19}F and ^{13}C -NMR spectra shown in the Supplementary Materials. All the synthesized compounds contained triflate (CF_3SO_3^-) as the counter anions were established from the HRESIMS data in negative ion mode and the peak of -79 ppm in the ^{19}F -NMR spectra. The ^1H -NMR signals at δ_{H} 1.40 (s, 9 H) and δ_{H} 7.64 (s, 2 H) could be attributed to the pyrylium motif. The trans-olefin was confirmed by the doublet olefinic proton signals with a coupling constant of 15.2 Hz.



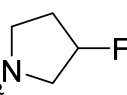
XY2 R = N(CH₃)₂

XY9 R = CO₂CH₃

XY15 R = 

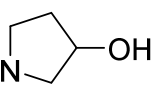
XY3 R = OCH₃

XY10 R = N(C₂H₅)₂

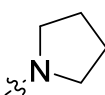
XY16 R = 

XY4 R = OH

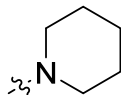
XY11 R = N,N-diphenyl

XY17 R = 

XY5 R = H

XY12 R = 

XY6 R = F

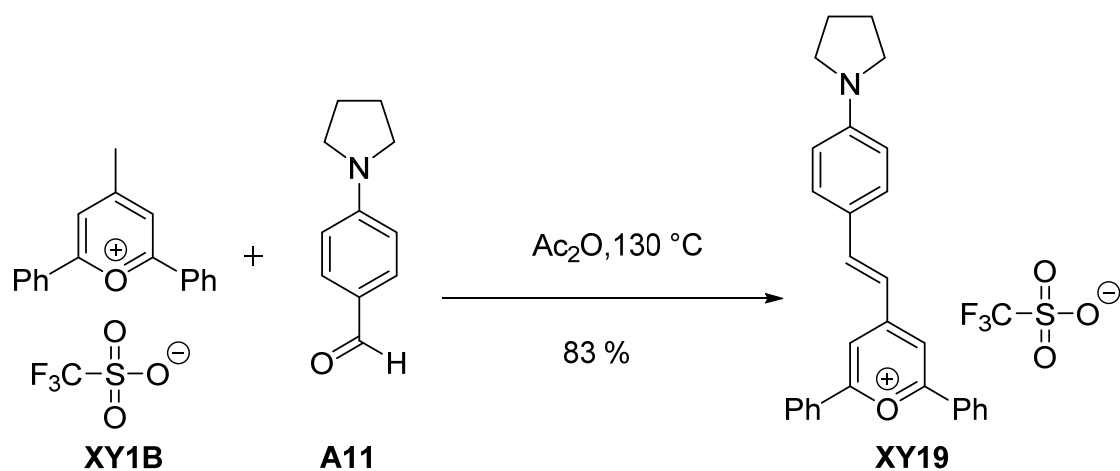
XY13 R = 

XY7 R = CN

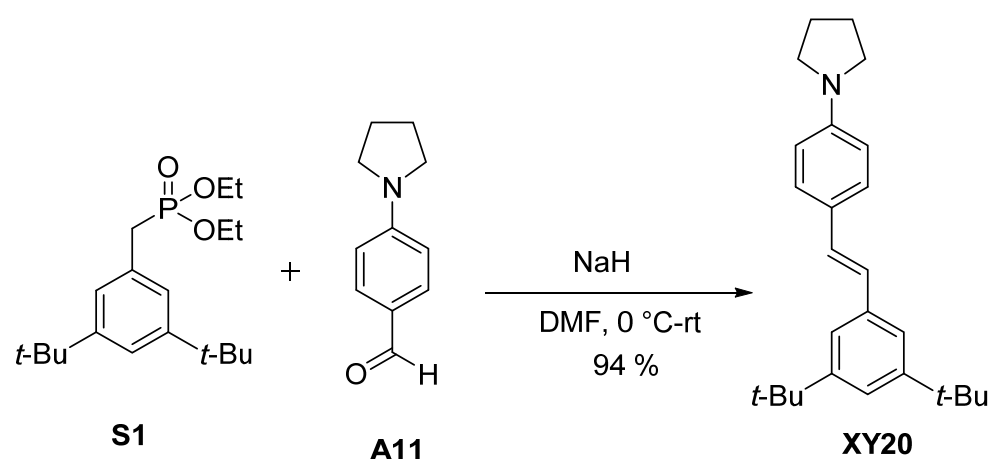
XY14 R = 

XY8 R = Ms

Scheme 1. The synthetic route for the target compounds XY2-17.



Scheme 2. The synthetic route for the target compound XY19.



Scheme 3. The synthetic route for the target compound **XY20**.

Moreover, the neutral analogue **XY20** was prepared by the Horner-Wadsworth-Emmons reaction. The treatment of aldehyde **A11** with dibenzyl phosphate **S1** under alkaline condition afforded *E*-type olefin **XY20** in a 94% yield (Scheme 3).

2.2. Structure-Activity Relationship (SAR) Studies

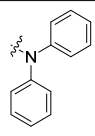
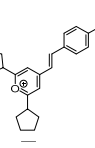
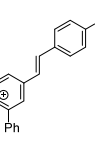
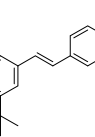
The main purpose of this study is to explore the chemical space and analyze the structure-activity relationship of pyrylium salt derivatives against fungi to find novel skeleton antimicrobial agents with high efficiency and low toxicity. A series of pyrylium salt derivatives were designed and synthesized and their antifungal activity was evaluated in vitro by standard pathogenic fungi *C. albicans* SC5314. These results are summarized in Table 1.

Firstly, the structure of **XY2** (**SM21**) was analyzed. Pyrylium salt (**XY1A**) and 4-(Dimethylamino)benzaldehyde (**A1**) showed no significant activity (MIC > 179.7 μM), which revealed that both fragments of the motif were required for antifungal activity. Pyrylium salt is a kind of cationic dye [14], in which the terminal groups have a dramatic effect on their properties, such as the properties of electron transition and spectral properties. Based on these properties, a series of pyrylium salt compounds (**XY2-17**) with different substituents were synthesized. Interestingly, a formal positive correlation between antifungal activity and spectral properties was observed. It is to be noted that the electron-donating levels, generated predominantly by terminal groups, certainly determined the antifungal activity. Compounds **XY7**, **XY8** and **XY9**, bearing a strong electron-withdrawing group, had no antifungal activity. At the same time, pyrylium salt derivatives without a substituent (**XY5**) or with a fluorine substituent (**XY6**) showed low activity, and the MIC was higher as 138.5 μM . As expected, the antifungal activity of methoxyl **XY3** (MIC = 67.5 μM) and phenolic hydroxyl **XY4** (MIC = 34.8 μM) were also much weaker than **XY2**. The above results prompted us to further study the substituent groups on nitrogen. By replacing dimethylamine (**XY2**) with diethylamine (**XY10**) and diphenylamine (**XY11**), the results showed the activity of diphenylamine decreased significantly and diethylamine (MIC = 0.49 μM) was equal to dimethylamine (MIC = 0.51 μM). Taken together, these results indicate that *N,N*-dialkylaniline as the terminal group is a necessary, but not sufficient, prerequisite for antifungal activity.

Next, a series of cyclic alkylamine derivatives were designed and synthesized for the antifungal evaluation (**XY12-15**). To our surprise, ring size was directly associated with the antifungal activity, with the five-membered ring being the most potent antifungal agent with an MIC value of 0.24 μM (**XY12**), whereas the activity of both four-membered and six-membered rings decreased (**XY13-14**, MIC = 0.95–1.0 μM). In addition, the introduction of a further heteroatoms such as morpholine, resulted in the decline in the activity (**XY15**, MIC = 3.8 μM). On this basis, the introduction of the fluoro-substituted and

hydroxyl-substituted derivatives (**XY16–17**) exhibited decreased activity (0.47 μM , 0.95 μM). It is possible that steric hindrance of substituents affects the activity of compounds. Thus far, we obtained the best compound, **XY12**.

Table 1. In vitro antifungal activities of the target compounds against pathogenic *C. albicans* SC5314.

Compounds	R	MIC (μM)	Compounds	R	MIC (μM)
XY1A	-	>179.7	XY11		>104.7
XY2	$\text{N}(\text{CH}_3)_2$	0.51	XY12		0.24
XY3	OCH_3	67.5	XY13		0.95
XY4	OH	34.8	XY14		1.0
XY5	H	144.1	XY15		3.8
XY6	F	138.5	XY16		0.47
XY7	CN	>136.4	XY17		0.94
XY8	SO_2CH_3	>122.6	XY18		8.7
XY9	COOCH_3	>127.4	XY19		3.6
XY10		0.49	XY20		>177.1

Finally, to evaluate the effect of substitutions on the pyrylium ring, the dicyclopentyl-substituted derivative **XY18** (commercially available) and diphenyl-substituted derivative **XY19** were synthesized, starting with the methyl pyrylium salt (**XY1B**) and aldehyde **A11** using the standard synthetic route described above (Scheme 2); they exhibited a decline in antifungal potency (8.7 and 3.6 μM , respectively) compared to *tert*-butyl-substituted counterparts (**XY2**, **XY12**). **XY20** was obtained by the Horner–Wadsworth–Emmons reaction (Scheme 3), and its pyrylium ring was replaced by a benzene ring. The inactivation of **XY20** (>177.1 μM) indicated the necessity of the cation (Table 1). This result further implied that this lipophilic pyrylium dye shows antifungal activity, probably via targeting mitochondria [12,13,16,17].

2.3. Pharmacological Activity of **XY12**

To further investigate the antifungal activity of **XY12**, a variety of *Candida* strains were used to test the MIC of **XY12** and **XY2**. Compared with the antifungal activity of **XY2**, the MIC of **XY12** decreased about one-fold. **XY12** showed enhanced antifungal bioactivity

against most of the tested *Candida* species with the MIC ranging from 0.12 μM to 0.97 μM , including *C. albicans*, *C. glabrata*, *C. tropicalis*, *C. krusei* and *C. parapsilosis* (Table 2). The compound **XY12** also showed excellent activity against fluconazole-resistant *C. albicans* 100 and 901 with the MIC value of 0.24 μM and 0.12 μM (Table 2). By comparing the radar charts, we clearly found that the MICs of **XY12** against the pathogenic *Candida* were lower than those of **XY2** (Figure 2), which indicated the stronger anti-*Candida* activities of **XY12**.

Table 2. Antifungal activity of **XY14** against *Candida*.

<i>Candida</i> Isolates	MIC (μM)		
	XY12	XY2	Fluconazole
<i>C. albicans</i> SC5314	0.24	0.51	0.82
<i>C. albicans</i> Y0109	0.24	0.51	0.40
<i>C. albicans</i> 100	0.24	1.0	>209.1
<i>C. albicans</i> 901	0.12	2.1	>209.1
<i>C. glabrata</i> 537	0.49	4.1	0.82
<i>C. glabrata</i> 896	0.97	2.1	1.6
<i>C. glabrata</i> 8535	0.24	2.1	6.5
<i>C. tropicalis</i> 753	0.24	2.1	1.6
<i>C. tropicalis</i> 112936	0.49	2.1	6.5
<i>C. tropicalis</i> 750	0.49	2.1	3.3
<i>C. parapsilosis</i> 90018	0.49	4.1	1.6
<i>C. parapsilosis</i> 22019	0.24	4.1	3.3
<i>C. parapsilosis</i> 700	0.24	2.1	6.5
<i>C. krusei</i> 463	0.97	1.0	13.1
<i>C. krusei</i> 629	0.97	2.1	6.5

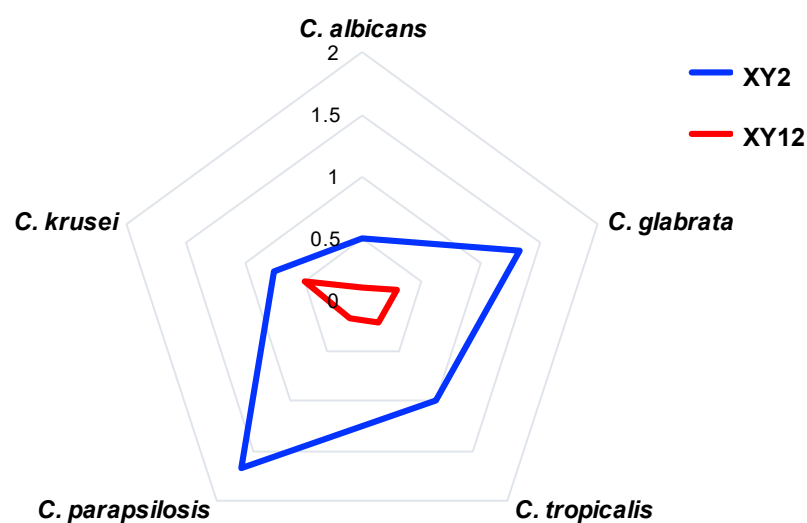


Figure 2. MICs of **XY12** and **XY2** against *Candida* species showed by Radar chart.

To investigate the cytotoxicity of **XY12** and **XY2**, the viability of human umbilical vein endothelial cells (HUVECs) was assayed by CCK-8 agents. As shown in Figure 3, 7.8 μM of **XY12** showed almost no toxicity to HUVECs and the IC_{50} of **XY12** was about 34.6 μM . However, a significant inhibitory effect of **XY2** was observed at the concentration of 0.51 μM . Meanwhile, the IC_{50} of **XY2** was about 1.8 μM , which indicated that the cytotoxicity of **XY12** was reduced by about 20-fold. Therefore, structural modification of **XY2** at the terminal groups not only improves the antifungal activity, but also reduces the cytotoxicity.

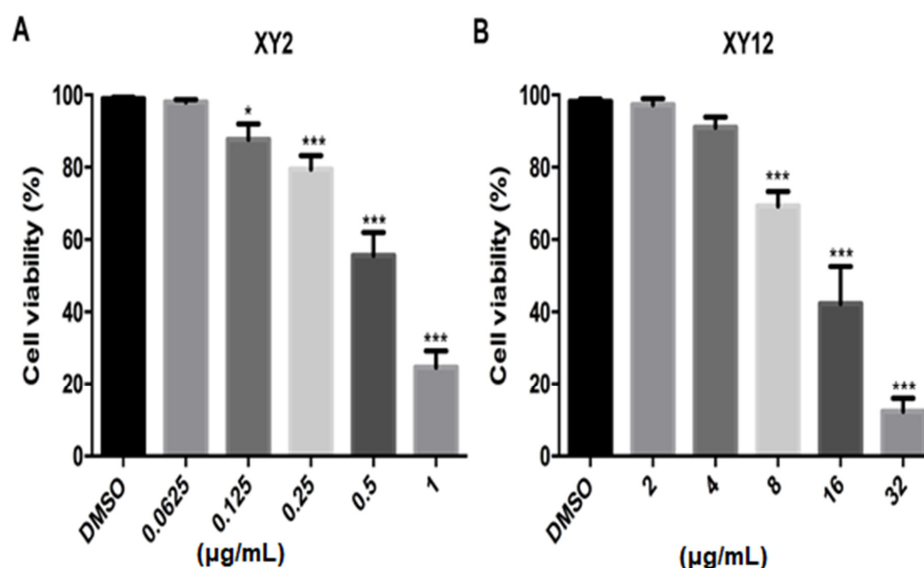


Figure 3. Cytotoxicity of compounds XY2 and XY12 detected by human umbilical vein endothelial cells (HUVECs). HUVECs were treated with different concentrations of compounds XY2 (A) and XY12 (B) for 24 h. Cell viability was detected by CCK-8 assay. Unpaired *t* test, * $p < 0.05$, *** $p < 0.001$.

Finally, we compared the in vivo antifungal activity of XY12 and XY2 using the systemic candidiasis model. Treated with 10 mg/kg of XY12, the average survival time and survival rate of mice increased significantly. However, XY2 did not show any protective efficacy against *C. albicans* infection at the dose of 10 mg/kg. When the dose reduced to 5 mg/kg, the protective effect of XY12 was lost. However, increasing the dose of XY12 not only failed to improve the protective effect, but also showed toxicity in vivo. The survival time of mice injected with 20 mg/kg of XY12 was shorter than that of mice injected with the solvent (Figure 4). Although XY12 showed moderate protective effect in vivo, it also caused abdominal irritation in mice, which was reflected by the writhing responses. Therefore, further structural modification of XY12 was required to enhance its antifungal effect and reduce its irritation to mammals.

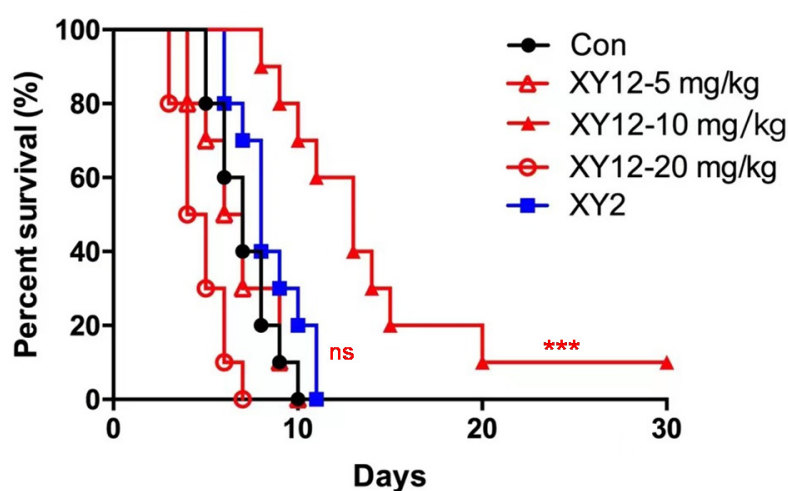


Figure 4. Survival of mice infected with *C. albicans* systemically. Female ICR mice were infected with *C. albicans* 1.5×10^6 CFU through tail vein; 10 mg/kg of XY2 or 5, 10, 20 mg/kg of XY12 was injected intraperitoneally once a day for 5 days and the survival of mice was observed for 30 days. Log-rank (Mantel–Cox) test, *** $p < 0.001$, ns—no significance.

3. Materials and Methods

3.1. Chemistry

3.1.1. General Information

All the starting materials were commercially available reagents and used without further purification. ^1H , ^{19}F and ^{13}C -NMR spectra were recorded at 500 MHz for ^1H , at 126 MHz for ^{13}C and at 282 MHz for ^{19}F in CDCl_3 with the BRUKER DRX-500 or 300M NMR spectrometer (Bruker, Billerica, MA, USA). Coupling constants were given in hertz (Hz). GC-MS was conducted using the Agilent MSD Trap XCT (for ESI) and Q-ToF (for HR-ESI-MS) (Agilent Technologies, Santa Clara, CA, USA) and were recorded on the Shimadzu/QP2010 Plus (Kyoto, Japan). All reactions were monitored by thin-layer chromatography (TLC) using silica-gel plates (silica gel 60 F254 0.25 mm).

3.1.2. Synthesis

This was the general procedure for the synthesis of **XY3-17**, **19**: To a mixture of **XY1A** or **XY1B** (0.168 mmol) and **A1-16** (0.202 mmol), acetic anhydride (1.0 mL) was added under an argon atmosphere. The mixture was allowed to stir at 130 °C for 3 h before it was cooled to room temperature and a precipitate formed. The precipitate was washed with diethyl ether (3×20 mL), which can be directly used or purified by flash column chromatography for purification to provide **XY3-17** (yield: 55–75%) and **XY19** (yield: 83%) as yellow or dark blue powder. The purity was identified by ^1H -NMR.

This was the general procedure for the synthesis of **XY20**: To a stirred solution of **S1** (0.176 mmol) in DMF, NaH (0.264 mmol) at 0 °C was added under an argon atmosphere. The mixture was allowed to stir at that temperature for 30 min before a solution of **A11** (0.211 mmol) in DMF was added. The mixture was allowed to stir at room temperature for 24 h before it was quenched with saturated aq. NaHCO_3 was extracted with EtOAc (3 times). The combined organic phases were washed with brine, dried over anhydrous Na_2SO_4 and filtered. The solvent was evaporated under vacuum, and the residue was subjected to flash column chromatography for purification using petroleum ether/EtOAc (10%) as eluent to give **XY20** (59.8 mg, yield: 94%) as a white powder.

XY3: An orange powder. Yield 71% (purity > 95%). ^1H -NMR (500 MHz, CDCl_3): δ = 8.42 (d, J = 16.1 Hz, 1 H), 7.92 (d, J = 8.8 Hz, 2 H), 7.85 (s, 2 H), 7.37 (d, J = 15.7 Hz, 1 H), 6.90 (d, J = 8.7, 2 H), 3.83 (d, J = 2.7 Hz, 3 H), 1.48 (d, J = 1.9 Hz, 18 H) ppm; ^{19}F -NMR (282 MHz, CDCl_3) δ = -78.7 ppm; ^{13}C -NMR (126 MHz, CDCl_3): δ = 183.0, 165.2, 164.4, 152.8, 133.7, 127.8, 120.8, 115.2, 113.2, 55.8, 38.6, 28.2 ppm. HRMS (m/z): $[\text{M}]^+$ calcd for $\text{C}_{22}\text{H}_{29}\text{O}_2^+$ 325.2162, found 325.2166; $[\text{M}]^-$ calcd for CF_3SO_3^- , 148.9526, found 148.9529.

XY4: An orange powder. Yield 59% (purity > 95%). ^1H -NMR (500 MHz, CDCl_3): δ = 9.36 (s, 1 H) 8.05 (d, J = 15.6 Hz, 1 H), 7.62–7.52 (m, 4 H), 7.05 (d, J = 15.7 Hz, 1 H), 6.88 (d, J = 8.3 Hz, 2 H), 1.48 (s, 18 H) ppm; ^{19}F -NMR (282 MHz, CDCl_3) δ = -78.7 ppm; ^{13}C -NMR (126 MHz, CDCl_3): δ = 183.5, 164.7, 162.3, 152.3, 133.5, 126.8, 119.5, 117.2, 112.4, 38.6, 28.0 ppm. HRMS (m/z): $[\text{M}]^+$ calcd for $\text{C}_{21}\text{H}_{27}\text{O}_2^+$ 311.2006, found 311.2012; $[\text{M}]^-$ calcd for CF_3SO_3^- , 148.9526, found 148.9528.

XY6: A brown powder. Yield 68% (purity > 95%). ^1H -NMR (500 MHz, CDCl_3): δ = 8.40 (d, J = 16.1 Hz, 1 H), 7.98 (dd, J = 8.9, 5.4 Hz, 2 H), 7.95 (s, 2 H), 7.44 (d, J = 16.0 Hz, 1 H), 7.08–7.02 (m, 2 H), 1.52 (s, 18 H) ppm; ^{19}F -NMR (282 MHz, CDCl_3) δ = -78.7 , -113.8 ppm; ^{13}C -NMR (126 MHz, CDCl_3): δ = 184.4, 165.7, 165.5 (d, J = 256.5 Hz), 151.0, 133.5 (d, J = 9.1 Hz), 131.10 (d, J = 2.9 Hz), 123.13 (d, J = 2.0 Hz), 116.70 (d, J = 21.9 Hz), 114.3, 38.9, 28.3 ppm. HRMS (m/z): $[\text{M}]^+$ calcd for $\text{C}_{21}\text{H}_{26}\text{FO}^+$ 313.1962, found 313.1972; $[\text{M}]^-$ calcd for CF_3SO_3^- , 148.9526, found 148.9527.

XY7: A brown powder. Yield 64% (purity > 95%). ^1H -NMR (500 MHz, CDCl_3): δ = 8.32 (d, J = 16.1 Hz, 1 H), 8.10 (s, 2 H), 8.00 (d, J = 8.0 Hz, 2 H), 7.61 (d, J = 8.2 Hz, 2 H), 7.58 (d, J = 16.2 Hz, 1 H), 1.54 (s, 18 H) ppm; ^{19}F -NMR (282 MHz, CDCl_3) δ = -78.7 ppm; ^{13}C -NMR (126 MHz, CDCl_3): δ = 186.0, 165.2, 148.2, 138.5, 132.9, 130.8, 126.2, 118.3, 115.4, 114.7, 39.2, 28.4. HRMS (m/z): $[\text{M}]^+$ calcd for $\text{C}_{22}\text{H}_{26}\text{NO}^+$ 320.2009, found 320.2015; $[\text{M}]^-$ calcd for CF_3SO_3^- , 148.9526, found 148.9530.

XY8: A brown powder. Yield 67% (purity > 95%). $^1\text{H-NMR}$ (500 MHz, CDCl_3): $\delta = 8.15$ (d, $J = 16.2$ Hz, 1 H), 8.05 (d, $J = 8.3$ Hz, 2 H), 8.00 (s, 2 H), 7.78 (d, $J = 8.1$ Hz, 2 H), 7.37 (d, $J = 16.2$ Hz, 1 H), 2.96 (s, 3 H), 1.56 (s, 18 H) ppm; $^{19}\text{F-NMR}$ (282 MHz, CDCl_3) $\delta = -78.7$ ppm; $^{13}\text{C-NMR}$ (126 MHz, CDCl_3): $\delta = 186.0, 164.7, 147.1, 142.1, 139.3, 131.3, 128.0, 126.0, 115.3, 44.3, 39.2, 28.3$ ppm. HRMS (m/z): $[\text{M}]^+$ calcd for $\text{C}_{22}\text{H}_{29}\text{O}_3\text{S}^+$ 373.1832, found 373.1839; $[\text{M}]^-$ calcd for CF_3SO_3^- , 148.9526, found 148.9527.

XY9: A yellow powder. Yield 72% (purity > 90%). $^1\text{H-NMR}$ (500 MHz, CDCl_3): $\delta = 8.41$ (d, $J = 16.1$ Hz, 1 H), 8.05 (s, 2 H), 7.99 (d, $J = 8.2$ Hz, 2 H), 7.96 (d, $J = 8.4$ Hz, 2 H), 7.63 (d, $J = 16.0$ Hz, 1 H), 3.91 (s, 3 H), 1.51 (s, 18 H) ppm; $^{19}\text{F-NMR}$ (282 MHz, CDCl_3) $\delta = -78.7$ ppm; $^{13}\text{C-NMR}$ (126 MHz, CDCl_3): $\delta = 185.3, 166.3, 165.5, 149.9, 138.5, 133.0, 130.4, 130.3, 125.6, 115.0, 52.5, 39.1, 28.3$ ppm. HRMS (m/z): $[\text{M}]^+$ calcd for $\text{C}_{23}\text{H}_{29}\text{O}_3^+$ 353.2111, found 353.2118; $[\text{M}]^-$ calcd for CF_3SO_3^- , 148.9526, found 148.9528.

XY10: A dark blue powder. Yield 59% (purity > 95%). $^1\text{H-NMR}$ (500 MHz, CDCl_3): $\delta = 8.23$ (d, $J = 15.0$ Hz, 1 H), 7.85 (d, $J = 8.7$ Hz, 2 H), 7.37 (s, 2 H), 7.06 (d, $J = 15.1$ Hz, 1 H), 6.74 (d, $J = 9.0$ Hz, 2 H), 3.50 (q, $J = 7.1$ Hz, 4 H), 1.42 (s, 18 H), 1.24 (t, $J = 7.1$ Hz, 6 H) ppm; $^{19}\text{F-NMR}$ (282 MHz, CDCl_3) $\delta = -78.7$ ppm; $^{13}\text{C-NMR}$ (126 MHz, CDCl_3): $\delta = 178.5, 160.7, 153.6, 153.2, 123.4, 116.1, 112.8, 45.5, 37.8, 28.2, 12.9$ ppm. HRMS (m/z): $[\text{M}]^+$ calcd for $\text{C}_{25}\text{H}_{31}\text{NO}^+$ 366.2791, found 366.2793; $[\text{M}]^-$ calcd for CF_3SO_3^- , 148.9526, found 148.9530.

XY11: A dark blue powder. Yield 57% (purity > 92%). $^1\text{H-NMR}$ (500 MHz, CDCl_3): $\delta = 8.35$ (d, $J = 15.4$ Hz, 1 H), 7.78 (d, $J = 8.7$ Hz, 2 H), 7.68 (s, 2 H), 7.37 (m, 4 H), 7.24–7.17 (m, 7 H), 6.96 (d, $J = 8.5$ Hz, 2 H), 1.48 (s, 18 H) ppm; $^{19}\text{F-NMR}$ (282 MHz, CDCl_3) $\delta = -78.7$ ppm; $^{13}\text{C-NMR}$ (126 MHz, CDCl_3): $\delta = 181.3, 163.5, 153.7, 152.9, 145.4, 133.8, 130.0, 127.0, 126.9, 126.2, 122.4, 119.8, 119.4, 119.1, 112.1, 38.4, 28.3$ ppm. HRMS (m/z): $[\text{M}]^+$ calcd for $\text{C}_{33}\text{H}_{36}\text{NO}^+$ 462.2791, found 462.2795; $[\text{M}]^-$ calcd for CF_3SO_3^- , 148.9526, found 148.9526.

XY12: A dark blue powder. Yield 75% (purity > 95%). $^1\text{H-NMR}$ (500 MHz, CDCl_3): $\delta = 8.23$ (d, $J = 15.0$ Hz, 1 H), 7.84 (d, $J = 8.5$ Hz, 2 H), 7.35 (s, 2 H), 7.06 (d, $J = 15.1$ Hz, 1 H), 6.64 (d, $J = 8.7$ Hz, 2 H), 3.50–3.47 (m, 4 H), 2.10–2.04 (m, 4 H), 1.42 (s, 18 H) ppm; $^{19}\text{F-NMR}$ (282 MHz, CDCl_3) $\delta = -78.6$ ppm; $^{13}\text{C-NMR}$ (126 MHz, CDCl_3): $\delta = 178.5, 160.6, 153.6, 153.1, 123.7, 122.2, 119.7, 116.1, 113.7, 48.5, 37.9, 28.2, 25.4$ ppm. HRMS (m/z): $[\text{M}]^+$ calcd for $\text{C}_{25}\text{H}_{34}\text{NO}^+$ 364.2635, found 364.2644; $[\text{M}]^-$ calcd for CF_3SO_3^- , 148.9526, found 148.9529.

XY 13: A dark blue powder. Yield 61% (purity > 95%). $^1\text{H-NMR}$ (500 MHz, CDCl_3): $\delta = 8.27$ (d, $J = 15.1$ Hz, 1 H), 7.86 (d, $J = 8.8$ Hz, 2 H), 7.45 (s, 2 H), 7.13 (d, $J = 15.1$ Hz, 1 H), 6.90 (d, $J = 8.7$ Hz, 2 H), 3.56 (m, 4 H), 1.73–1.69 (m, 6 H), 1.44 (s, 18 H) ppm; $^{19}\text{F-NMR}$ (282 MHz, CDCl_3) $\delta = -78.7$ ppm; $^{13}\text{C-NMR}$ (126 MHz, CDCl_3): $\delta = 183.7, 164.0, 149.4, 133.0, 122.7, 121.7, 119.5, 118.9, 113.6, 54.8, 38.8, 28.2, 24.1, 22.1$ ppm. HRMS (m/z): $[\text{M}]^+$ calcd for $\text{C}_{26}\text{H}_{36}\text{NO}^+$ 378.2791, found 378.2792; $[\text{M}]^-$ calcd for CF_3SO_3^- , 148.9526, found 148.9529.

XY14: A dark blue powder. Yield 63% (purity > 95%). $^1\text{H-NMR}$ (500 MHz, CDCl_3): $\delta = 8.22$ (d, $J = 15.2$ Hz, 1 H), 7.81 (d, $J = 8.4$ Hz, 2 H), 7.37 (s, 2 H), 7.05 (d, $J = 15.1$ Hz, 1 H), 6.37 (d, $J = 8.6$ Hz, 2 H), 4.14 (t, $J = 7.5$ Hz, 4 H), 2.48 (m, 2 H), 1.42 (s, 18 H) ppm; $^{19}\text{F-NMR}$ (282 MHz, CDCl_3) $\delta = -78.7$ ppm; $^{13}\text{C-NMR}$ (126 MHz, CDCl_3): $\delta = 178.7, 160.8, 155.0, 153.6, 123.9, 116.2, 111.2, 51.5, 37.9, 28.2, 16.2$ ppm. HRMS (m/z): $[\text{M}]^+$ calcd for $\text{C}_{24}\text{H}_{32}\text{NO}^+$ 350.2478, found 350.2484; $[\text{M}]^-$ calcd for CF_3SO_3^- , 148.9526, found 148.9530.

XY15: A dark blue powder. Yield 67% (purity > 90%). $^1\text{H-NMR}$ (500 MHz, CDCl_3): $\delta = 8.32$ (d, $J = 15.2$ Hz, 1 H), 7.89 (d, $J = 8.5$ Hz, 2 H), 7.60 (s, 2 H), 7.24 (d, $J = 16.3$ Hz, 1 H), 6.92–6.86 (m, 1 H), 3.88–3.75 (m, 1 H), 3.5–3.39 (m, 1 H), 1.45 (s, 18 H) ppm; $^{19}\text{F-NMR}$ (282 MHz, CDCl_3) $\delta = -78.7$ ppm; $^{13}\text{C-NMR}$ (126 MHz, CDCl_3): $\delta = 180.7, 163.0, 154.9, 153.2, 134.7, 125.2, 118.3, 114.0, 111.5, 66.5, 46.9, 38.2, 28.2$ ppm. HRMS (m/z): $[\text{M}]^+$ calcd for $\text{C}_{25}\text{H}_{34}\text{NO}_2^+$ 380.2584, found 380.2589; $[\text{M}]^-$ calcd for CF_3SO_3^- , 148.9526, found 148.9523.

XY16: A dark blue powder. Yield 63% (purity > 92%). $^1\text{H-NMR}$ (500 MHz, CDCl_3): $\delta = 8.30$ (d, $J = 15.0$ Hz, 1 H), 7.87 (d, $J = 8.5$ Hz, 2 H), 7.47 (s, 2 H), 7.14 (d, $J = 15.0$ Hz, 1 H), 6.59 (d, $J = 8.3$ Hz, 2 H), 5.42 (d, $J = 52.0$ Hz, 1 H), 3.72–3.54 (m, 4 H), 2.49–2.35 (m, 1 H), 2.29–2.11 (m, 1 H), 1.43 (s, 18 H) ppm; $^{19}\text{F-NMR}$ (282 MHz, CDCl_3) $\delta = -78.7, -173.5, -179.0$

(m) ppm; ^{13}C -NMR (126 MHz, CDCl_3): $\delta = 179.3, 161.7, 153.7, 152.5, 124.1, 122.3, 119.8, 116.8, 113.5, 92.39$ (d, $J = 176.4$ Hz), 54.80 (d, $J = 23.1$ Hz), $46.0, 38.0, 32.05$ (d, $J = 21.8$ Hz), 28.2 ppm. HRMS (m/z): $[\text{M}]^+$ calcd for $\text{C}_{25}\text{H}_{33}\text{FNO}^+$ 382.2541, found 382.2544; $[\text{M}]^-$ calcd for CF_3SO_3^- , 148.9526, found 148.9523.

XY17: A dark blue powder. Yield 55% (purity > 92%). ^1H -NMR (500 MHz, CDCl_3): $\delta = 8.33$ (d, $J = 15.0$ Hz, 1 H), 7.90 (d, $J = 8.5$ Hz, 2 H), 7.49 (s, 2 H), 7.16 (d, $J = 15.0$ Hz, 1 H), 6.65 (d, $J = 8.4$ Hz, 2 H), 5.46 (d, $J = 4.0$ Hz, 1 H), 3.75 (dd, $J = 12.5, 4.7$ Hz, 1 H), 3.67 – 3.59 (m, 2 H), 3.56 (d, $J = 12.5$ Hz, 1 H), 2.30 – 2.25 (m, 2 H), 1.45 (s, 18 H) ppm; ^{19}F -NMR (282 MHz, CDCl_3) $\delta = -78.6$ ppm; ^{13}C -NMR (126 MHz, CDCl_3): $\delta = 179.4, 161.7, 153.8, 152.5, 124.1, 122.3, 119.7, 116.9, 113.5, 73.2, 54.0, 46.3, 38.0, 31.1, 28.3$ ppm. HRMS (m/z): $[\text{M}]^+$ calcd for $\text{C}_{25}\text{H}_{34}\text{NO}_2^+$ 380.2584, found 380.2590; $[\text{M}]^-$ calcd for CF_3SO_3^- , 148.9526, found 148.9528.

XY19: A dark blue powder. Yield 83% (purity > 95%). ^1H -NMR (500 MHz, CDCl_3): $\delta = 8.31$ (s, 2 H), 8.25 (d, $J = 15.8$ Hz, 1 H), 8.20 (d, $J = 7.7$ Hz, 4H), 7.94 (d, $J = 8.2$ Hz, 2 H), 7.82 – 7.78 (m, 2 H), 7.75 – 7.66 (m, 4 H), 7.53 (d, $J = 8.1$ Hz, 2 H), 7.47 (d, $J = 15.8$ Hz, 1 H), 3.87 – 3.76 (m, 4 H), 2.37 – 2.29 (m, 4 H) ppm; ^{19}F -NMR (282 MHz, CDCl_3) $\delta = -78.6$ ppm; ^{13}C -NMR (126 MHz, CDCl_3): $\delta = 169.6, 160.4, 147.9, 144.6, 135.7, 132.6, 130.5, 128.7, 128.0, 123.6, 121.0, 118.6, 113.8, 57.9, 24.3$ ppm. HRMS (m/z): $[\text{M}]^+$ calcd for $\text{C}_{29}\text{H}_{26}\text{NO}^+$ 404.2009, found 404.2014; $[\text{M}]^-$ calcd for CF_3SO_3^- , 148.9526, found 148.9528.

XY20: A white powder. Yield 94% (purity > 95%). ^1H -NMR (300 MHz, CDCl_3): $\delta = 7.44$ (d, $J = 8.6$ Hz, 2 H), 7.36 – 7.33 (m, 2 H), 7.31 (m, 1 H), 7.06 (d, $J = 16.2$ Hz, 1 H), 6.95 (d, $J = 16.2$ Hz, 1 H), 6.59 (d, $J = 8.2$ Hz, 2 H), 3.45 – 3.27 (m, 4 H), 2.18 – 1.91 (m, 4 H), 1.38 (s, 18 H) ppm; ^{13}C -NMR (75 MHz, CDCl_3): $\delta = 151.0, 147.5, 137.5, 128.5, 127.8, 125.0, 121.2, 120.5, 112.0, 47.8, 35.0, 31.6, 25.6$ ppm. HRMS (m/z): $[\text{M} + \text{H}]^+$ calcd for $\text{C}_{25}\text{H}_{35}\text{N}^+$ 362.2842, found 362.2841.

3.2. In Vitro Antifungal Activity

The standard *C. albicans* SC5314 was donated by Professor William A. Fonzi of Georgetown University in the United States. Clinical isolates of *C. albicans*, *C. glabrata*, *C. tropicalis*, *C. krusei* and *C. parapsilosis* were isolated from patients of Changhai Hospital and identified by biochemistry and morphology. The antifungal minimum inhibitory concentration (MIC) was measured by serial dilution in 96-well plates with RPMI 1640 medium as described in the Clinical and Laboratory Standards Institute (CLSI) guidelines (CLSI M27-A3). The MIC is defined as the concentration that reduced fungal growth by more than 95%. All compounds were dissolved in DMSO. The OD_{600} was determined after *Candida* was cultured at 30°C for 48 h. The MIC of each compound was calculated by OD_{600} . All the antifungal activity was detected at least two times. The in vitro antifungal activities of **XY1A–20** were evaluated by the *C. albicans* standard isolate SC5314.

3.3. Cytotoxicity against Human Umbilical Vein Endothelial Cells (HUVECs)

HUVECs were cultured to detect the cytotoxicity of **XY12** and **XY2** as described. HUVECs were cultured in DMEM containing 10% fetal bovine serum (FBS). Then, a $100\ \mu\text{L}$ suspension of HUVECs (1×10^5 cells/mL) was added to 96-well tissue culture plates and incubated at 37°C for 3 h. After incubation, the supernatant was replaced by $100\ \mu\text{L}$ of fresh DMEM complete mediums containing different concentrations of **XY12** and **XY2**. After incubation for 24 h, the supernatant was added with $10\ \mu\text{L}$ of CCK-8 agents and cultured at 37°C for 2 h. Finally, cell viability was assessed by measuring OD_{450} [18].

3.4. In Vivo Antifungal Activity

8-week-old female ICR mice were purchased from Shanghai SLAC Laboratory Animal Co., Ltd (Shanghai, China). The mice were injected with a $200\ \mu\text{L}$ PBS suspension of *C. albicans* SC5314 (7.5×10^6 CFU/mL) through the tail vein. **XY12** and **XY2** compounds were solved in the DPH buffer (5% DMSO, 30% PEG 400 and 65% ddH₂O) and injected intraperitoneally 2 h after infection. **XY12** and **XY2** were injected in the mice once a day for 5 days. After that, the mice were observed daily for survival.

4. Conclusions

In summary, based on the lead compound **SM21 (XY2)**, we synthesized a series of pyrylium salt derivatives and evaluated their antifungal activities. Most of the designed compounds exhibited moderate in vitro antifungal activities against *C. albicans*. Among them, the most promising antifungal agent was coded as **XY12**. Compared with the lead compound **XY2**, **XY12** showed lower cytotoxicity and higher activity against *Candida* species, including the fluconazole-resistant *C. albicans*. Additionally, the in vivo antifungal activity of **XY12** was also enhanced. The SARs study demonstrated that the electron-donating level of terminal groups on the benzene ring determined antifungal activity. At the same time, further activity and selectivity strongly depended on the ring size and steric hindrance of terminal cyclic alkylamine. The character of lipophilic cations responsible for activity implies that this type of pyrylium dye exhibited the antifungal activity, probably via targeting mitochondria. Researches on the antifungal mechanisms of pyrylium salts will provide more information for further structural modifications.

Supplementary Materials: The following supporting information can be downloaded at: <https://www.mdpi.com/article/10.3390/molecules27144450/s1>, The copies of ^1H NMR, ^{19}F NMR and ^{13}C NMR spectra, HRMS for all new synthesized compounds.

Author Contributions: Conceptualization, J.W., Q.L. (Quanzhen Lv) and R.L.; methodology, Y.Q.; software, Y.Z., Q.L. (Qiu hao Li) and W.C.; validation, J.W. and Q.L. (Quanzhen Lv); investigation, Y.Z., Q.L. (Qiu hao Li) and W.C.; J.C. and Y.W., writing—original draft preparation, Y.Z., J.W. and Q.L. (Quanzhen Lv); funding acquisition, Q.L. (Quanzhen Lv) and J.W. All authors have read and agreed to the published version of the manuscript.

Funding: This work was supported by the National Natural Science Foundation of China (Nos. 82003624, J.W., 81902039, Q.L.) and the Science and Technology Commission of Shanghai Municipality (Nos. 20YF1458700, J.W.).

Institutional Review Board Statement: The animal study protocol was approved by the Committee on Ethics of Medicine, Navy Medical University.

Informed Consent Statement: Not applicable.

Data Availability Statement: Not applicable.

Acknowledgments: We are grateful to Lu Lu for carrying out the NMR experiments.

Conflicts of Interest: The authors declare no conflict of interest.

Sample Availability: Samples of the compounds are available from the authors.

References

1. Jermy, A. Stop neglecting fungi. *Nat. Microbiol.* **2017**, *2*, 17120. [[CrossRef](#)]
2. Brown, G.D.; Denning, D.W.; Gow, N.A.; Levitz, S.M.; Netea, M.G.; White, T.C. Hidden killers: Human fungal infections. *Sci. Transl. Med.* **2012**, *4*, 165rv13. [[CrossRef](#)] [[PubMed](#)]
3. Sakagami, T.; Kawano, T.; Yamashita, K.; Yamada, E.; Fujino, N.; Kaeriyama, M.; Fukuda, Y.; Nomura, N.; Mitsuyama, J.; Suematsu, H.; et al. Antifungal susceptibility trend and analysis of resistance mechanism for *Candida* species isolated from bloodstream at a Japanese university hospital. *J. Infect. Chemother.* **2019**, *25*, 34–40. [[CrossRef](#)] [[PubMed](#)]
4. Kullberg, B.J.; Arendrup, M.C. Invasive Candidiasis. *N. Engl. J. Med.* **2015**, *373*, 1445–1456. [[CrossRef](#)] [[PubMed](#)]
5. Berman, J.; Krysan, D.J. Drug resistance and tolerance in fungi. *Nat. Rev. Microbiol.* **2020**, *18*, 319–331. [[CrossRef](#)] [[PubMed](#)]
6. White, P.L.; Dhillon, R.; Hughes, H.; Wise, M.P.; Backx, M. COVID-19 and fungal infection: The need for a strategic approach. *Lancet Microbe* **2020**, *1*, e196. [[CrossRef](#)]
7. Bongomin, F.; Gago, S.; Oladale, R.O.; Denning, D.W. Global and multinational prevalence of fungal diseases: Estimate precision. *J. Fungi* **2017**, *3*, 57. [[CrossRef](#)] [[PubMed](#)]
8. Mourad, A.; Perfect, J.R. Tolerability profile of the current antifungal armoury. *J. Antimicrob. Chemother.* **2018**, *73*, i26–i32. [[CrossRef](#)] [[PubMed](#)]
9. Hendrickson, J.A.; Hu, C.; Aitken, S.L.; Beyda, N. Antifungal Resistance: A Concerning Trend for the Present and Future. *Curr. Infect. Dis. Rep.* **2019**, *21*, 47. [[CrossRef](#)] [[PubMed](#)]
10. Liu, W.; Tan, J.; Sun, J.; Xu, Z.; Li, M.; Yang, Q.; Shao, H.; Zhang, L.; Liu, W.; Wan, Z.; et al. Invasive candidiasis in intensive care units in China: In vitro antifungal susceptibility in the China-SCAN study. *J. Antimicrob. Chemother.* **2014**, *69*, 162–167. [[CrossRef](#)] [[PubMed](#)]

11. Wong, S.S.; Kao, R.Y.; Yuen, K.Y.; Wang, Y.; Yang, D.; Samaranyake, L.P.; Seneviratne, C.J. In vitro and in vivo activity of a novel antifungal small molecule against *Candida* infections. *PLoS ONE* **2014**, *9*, e85836.
12. Truong, T.; Suriyanarayanan, T.; Zeng, G.; Le, T.D.; Liu, L.; Li, J.; Tong, C.; Wang, Y.; Seneviratne, C.J. Use of Haploid Model of *Candida albicans* to Uncover Mechanism of Action of a Novel Antifungal Agent. *Front. Cell. Infect. Microbiol.* **2018**, *8*, 164. [[CrossRef](#)] [[PubMed](#)]
13. Truong, T.; Zeng, G.; Lim, T.K.; Cao, T.; Pang, L.M.; Lee, Y.M.; Lin, Q.; Wang, Y.; Seneviratne, C.J. Proteomics Analysis of *Candida albicans* dnm1 Haploid Mutant Unraveled the Association between Mitochondrial Fission and Antifungal Susceptibility. *Proteomics* **2020**, *20*, e1900240. [[CrossRef](#)] [[PubMed](#)]
14. Bricks, J.L.; Stanova, A.V.; Ryabitsky, A.B.; Yashchuk, V.M.; Kachkovsky, A.D. Studies of 2-azaazulenium derivatives-3: The nature of electron transitions and spectral properties of styryl dyes containing terminal groups of different types. *J. Mol. Struct.* **2013**, *1033*, 215–226. [[CrossRef](#)]
15. Balaban, T.S.; Balaban, A.T. Product Class 1: Pyrylium Salts. In *Science of Synthesis*, 1st ed.; Thomas, E.J., Ed.; Thieme: Stuttgart, Germany, 2003; pp. 11–200.
16. Li, D.; Calderone, R. Exploiting mitochondria as targets for the development of new antifungals. *Virulence* **2017**, *8*, 159–168. [[CrossRef](#)] [[PubMed](#)]
17. Chang, W.; Liu, J.; Zhang, M.; Shi, H.; Zheng, S.; Jin, X.; Gao, Y.; Wang, S.; Ji, A.; Lou, H. Efflux pump-mediated resistance to antifungal compounds can be prevented by conjugation with triphenylphosphonium cation. *Nat. Commun.* **2018**, *9*, 5102. [[CrossRef](#)] [[PubMed](#)]
18. Lu, R.Y.; Ni, T.J.H.; Wu, J.; Yan, L.; Lv, Q.Z.; Li, L.P.; Zhang, D.Z.; Jiang, Y.Y. New Triazole NT-a9 Has Potent Antifungal Efficacy against *Cryptococcus neoformans* In Vitro and In Vivo. *Antimicrob. Agents Chemother.* **2020**, *64*, e01628-19. [[CrossRef](#)] [[PubMed](#)]